Development of Anthropometric Specifications for the Warrior Injury Assessment Manikin (WIAMan)

Matthew P. Reed

Biosciences Group
University of Michigan Transportation Research Institute

October 2013

Development of Anthropometric Specifications for the Warrior Injury Assessment Manikin (WIAMan)

Final Report

UMTRI-2013-38

by

Matthew P. Reed

University of Michigan Transportation Research Institute

October 2013

REPORT DOCUMENTATION PAGE

Form Approved
OMB No. 0704-0188

1. REPORT DATE *(DD-MM-YYYY)*	2. REPORT TYPE	3. DATES COVERED *(From - To)*
October 31, 2013	Final Report	September 2011- October 2013

4. TITLE AND SUBTITLE

Development of Anthropometric Specifications for the Warrior Injury Assessment Manikin (WIAMan)

5a. CONTRACT NUMBER
W56HZV-04-2-0001 P00038

5b. GRANT NUMBER

5c. PROGRAM ELEMENT NUMBER

6. AUTHOR(S)

Reed, Matthew P.

5d. PROJECT NUMBER

5e. TASK NUMBER

5f. WORK UNIT NUMBER

7. PERFORMING ORGANIZATION NAME(S) AND ADDRESS(ES)

University of Michigan
Transportation Research Institute

8. PERFORMING ORGANIZATION REPORT

UMTRI-2013-38

9. SPONSORING / MONITORING AGENCY NAME(S) AND ADDRESS(ES)

US Army Tank Automotive Research,
Development, and Engineering Center

Warren, MI 48397-5000

10. SPONSOR/MONITOR'S ACRONYM(S)

11. SPONSOR/MONITOR'S REPORT NUMBER(S)
Issued Upon Submission

12. DISTRIBUTION / AVAILABILITY STATEMENT

13. SUPPLEMENTARY NOTES

14. ABSTRACT

Data from a previous study of soldier posture and body shape were analyzed to develop anthropometric specifications for the Warrior Injury Assessment Manikin (WIAMan), an anthropomorphic test device (ATD) intended to represent a midsize male soldier for assessments of vehicle occupant protection in underbody blast. Target stature, body mass, and erect sitting height were established by reference to the median values for these dimensions in a recent Army study. Body landmark locations from 100 soldiers with a wide range of body size obtained in a single squad seating condition were analyzed using regression methods to establish target surface landmark and internal joint center locations. Laser scan data from 126 men in up to four seated postures were analyzed using principal component analysis and regression to obtain a statistical model predicting body shape as a function of overall body dimensions and surface landmark locations. A subset of the target landmarks obtained in the squad posture analysis were used as input to the body shape model, resulting in a three-dimensional representation of the mean expected body shape for soldiers matching the target body dimensions in the reference seating condition. Small adjustments to the posture and shape were made to obtain a symmetrical posture with the thighs horizontal and legs vertical. Additional analyses of posture and CT data were conducted to estimate spine segment orientations and pelvis geometry.

15. SUBJECT TERMS
Anthropometry, Posture, Vehicle Occupants, Statistical Shape Analysis, Safety

16. SECURITY CLASSIFICATION OF:			17. LIMITATION OF ABSTRACT	18. NUMBER OF PAGES	19a. NAME OF RESPONSIBLE PERSON M.P. Reed
a. REPORT	b. ABSTRACT	c. THIS PAGE		38	19b. TELEPHONE NUMBER *(include area code)*
UNCLASSIFIED, Dist A.	UNCLASSIFIED, Dist A.	UNCLASSIFIED, Dist A.			(734)936-1111

Standard Form 298 (Rev. 8-98)
Prescribed by ANSI Std. Z39.18

ACKNOWLEDGMENTS

This work was supported by the Automotive Research Center, a U.S. Army Center of Excellence for Modeling and Simulation of Ground Vehicles led by the University of Michigan.

This research would not have been possible without the contributions of a large number of people. We would like to thank the soldiers who participated in the Seated Soldier Study, providing valuable data that will improve safety and accommodation for the next generation of soldiers. The project was conducted in close collaboration with personnel from the U.S. Army Tank Automotive Research, Development and Engineering Center (TARDEC). Hollie Pietsch was the primary technical point of contact for this analysis. Katrina Harris was the primary technical point of contact for the Seated Soldier Study, on which this analysis was based. At UMTRI, Sheila Ebert conducted much of the data analysis. Dr. Brian Corner of the U.S. Army Natick Soldier Research, Development, and Engineering Center provided valuable input. The work was conducted collaboratively with the WIAMan ATD development team. Thanks goes to Jerry Wang and his group at Humanetics Innovative Solutions, who used the information developed in this effort as input to the WIAMan ATD design.

CONTENTS

ABSTRACT

Data from a previous study of soldier posture and body shape were analyzed to develop anthropometric specifications for the Warrior Injury Assessment Manikin (WIAMan), an anthropomorphic test device (ATD) intended to represent a midsize male soldier for assessments of vehicle occupant protection in underbody blast. Target stature, body mass, and erect sitting height were established by reference to the median values for these dimensions in a recent Army study. Body landmark locations from 100 soldiers with a wide range of body size obtained in a single squad seating condition were analyzed using regression methods to establish target surface landmark and internal joint center locations. Laser scan data from 126 men in up to four seated postures were analyzed using principal component analysis and regression to obtain a statistical model predicting body shape as a function of overall body dimensions and surface landmark locations. A subset of the target landmarks obtained in the squad posture analysis were used as input to the body shape model, resulting in a three-dimensional representation of the mean expected body shape for soldiers matching the target body dimensions in the reference seating condition. Small adjustments to the posture and shape were made to obtain a symmetrical posture with the thighs horizontal and legs vertical. Additional analyses of posture and CT data were conducted to estimate spine segment orientations and pelvis geometry.

INTRODUCTION

The Warrior Injury Assessment Manikin (WIAMan) program aims to develop a new anthropomorphic test device (ATD) for use in underbody blast testing of military vehicles and vehicle components. The new ATD is intended to provide more realistic posture, seat interaction, and dynamic response for these loading modes and for military seating scenarios than the Hybrid-III family of ATDs that are currently used.

The midsize-male WIAMan will represent a male soldier with median stature and body weight for the current Army. The goal of the work described in this report is to specify the posture, body shape, and skeletal linkage dimensions for this reference person. The specification of body segment inertial parameter values is not part of the current effort.

Previous ATD development programs have used two general approaches to developing anthropometric specifications. The dimensions of the Hybrid-III family were chosen from tabulations of standard anthropometric dimensions (lengths, breadths, and circumferences) obtained in unrelated studies of civilian anthropometry (Mertz et al. 2001). A small amount of information on seated posture and pelvis geometry was obtained from measurements of a few individuals similar in size to the ATD (Backaitis and Mertz 1994).

The Anthropometry of Motor Vehicle Occupants (AMVO) study, conducted at the University of Michigan Transportation Research Institute (UMTRI) in the early 1980s, gathered anthropometric data specifically for purposes of ATD development (Schneider et al. 1983). Overall reference body dimensions (stature, body weight, and erect sitting height) were identified from the target percentiles of tabulated data for the U.S. adult population. Individuals who were close in size to the three target ATD sizes (small female, midsize male, large male) were recruited for detailed study. In the first phase, driving postures were recorded in real vehicle seats by measuring the three-dimensional locations of body landmarks using stereophotogrammetry. In the second phase, body landmark locations were measured for twenty-five men or women in each category as they sat in a specially prepared rigid seat that allowed access to posterior as well as anterior torso landmarks. A small number of linear body contour measurements were made using a manual contour gage. Photography was used extensively to document body shape.

The means of the body landmark coordinates for each subject size group were taken as the specifications for the associated ATD. Additional manual measurements of the seated subjects taken using standard anthropometric techniques were included as part of the specification. The surface landmarks were used to estimate internal joint locations based on previous cadaveric studies. A set of three full-size surface shells (small female, midsize male, large male) were created based on the landmark measures, standard anthropometric data, linear contour measurements, and photographs. These surface shells formed a critical part of the specification, filling in

the gaps between the landmarks with contour information. The AMVO data have been used for the development of several ATDs, notably the midsize-male and small-female THOR and WorldSID ATDs (Moss et al. 2000, McDonald et al. 2003).

The current analysis is similar to the AMVO approach except that modern measurement methodology and advances in statistical methods have allowed a more general and complete analysis. As with AMVO, target values for reference dimensions (stature, body weight, and erect sitting height) were obtained from previous studies of the relevant population. However, instead of measuring only individuals similar in size to the ATD, posture measurements were made for a diverse sample of individuals with a wide range of body size in a range of vehicle-seat conditions. In addition to three-dimensional surface landmark measurements, whole-body surface coordinate data were obtained using a VITUS XXL whole-body laser scanner (Human Solutions). Skeletal joint locations were estimated from surface landmarks using techniques similar to AMVO, except that more complete data on pelvis geometry from medical imaging data were used. The target configuration of landmarks and joints was computed using linear regression analysis with the reference anthropometric dimensions as predictors.

A statistical model of the whole body surface was generated by fitting a homologous template mesh to each body scan, conducting a principal component analysis on the mesh vertices to reduce the dimension of the data, and creating a linear regression model to predict mesh vertex locations from standard anthropometric variables and body landmark locations. The body surface target for the ATD was created by using the reference body dimensions and landmark locations predicted from the vehicle-seat data as input to the body shape model. The resulting shape and landmark data were adjusted for use as the WIAMan specification by articulating the lower extremities using non-rigid morphing techniques.

Following completion of the anthropometric specifications for the ATD, a broader set of data from the squad conditions in the Seated Soldier Study were analyzed to provide guidance for biomechanics testing in support of the WIAMan program. Soldier posture data from four conditions were analyzed using regression methods to estimate the effects of seat back angle change on the orientation of torso body segments. Medical imaging data were analyzed to estimate spine segment orientations from the surface landmark data and to calculate pelvis size and shape.

Table 1 provides an overview of the various analyses that are presented in this report, their data sources, and the outcomes reported below. The motivation for each analysis is listed briefly – see the text for more detail. This report describes the data analysis methodology and results. The data collection and processing methods are described separately in Reed and Ebert (2013).

Table 1
Summary of Objectives, Methods, and Outcomes

Objective	Data Source	Analysis Method	Outcome
1. Posture analysis for the WIAMan anthropometry target	Body landmark locations measured in Seated Soldier Study, squad condition C01 (N=100)	Regression using target stature, body weight, and ratio of sitting height to stature	Tabular data on landmark and joint locations
2. External body shape for WIAMan ATD	Whole-body laser scan data in minimally clad condition, up to four seated postures per participant (N=126)	Surface template fitting followed by principal component and regression analyses	Body surface described by a polygonal mesh with 30004 corresponding to the target body dimensions and landmark locations from Objective 1
3. Male pelvis geometry	CT image analysis (N=49)	Regression analysis of landmark locations	Target landmarks and polygonal surface mesh for WIAMan pelvis
4. Effects of gear ensemble on torso posture	Seated Soldier Study, squad conditions C01 (N=92 to 100, depending on gear ensemble level)	Regression on landmark locations and segment orientations	Predictions of torso segment orientations across gear ensemble levels
5. Relationships among T12, L5, and S1 spine segments and pelvis	CT image analysis (N=31)	Analysis of relative segment orientations	Mean side-view angle offset between pelvis orientation and S1 superior surface
6. Effects of seat and soldier factors on torso posture	Seated Soldier Study, squad conditions C01, C02, C05, and C07 (N=47 to 121, depending on condition)	Regression analysis on body segment orientations and landmark locations	Regression models predicting the effects of seat and soldier factors, including gear ensemble, on torso posture

METHODS

Reference Anthropometry

Following many previous ATD development efforts, the WIAMan target is the "average" or "median" male for the population (in this case, U.S. Army soldiers). The reference database was originally identified as ANSUR II, but ANSUR II data were not available at the time of the analysis. Consequently, the ANSUR II Pilot study was chosen to provide the reference dimensions (Paquette et al. 2009). Median values of stature, body weight, and erect sitting height were selected to define the "median male." Stature is the best measure of overall body size. Body weight accounts for adiposity and muscular development, and erect sitting height accounts for the relationship between limb length and torso length, which varies on average across race/ethnicity groups. Table 2 list the targets for WIAMan from ANSUR II Pilot (A2P) as well as values from AMVO and ANSUR 88 (Gordon et al. 1989). For AMVO, both the sampling target values obtained from national civilian data and the summary statistics of the actual study participants are reported. The current target values differ substantially from AMVO and ANSUR 88 only in the larger body mass (5 kg greater than ANSUR 88 and 7 kg greater than AMVO).

Table 2
Male Reference Dimensions Compared with Previous Studies

Dimension (50th-percentile values)	WIAMan Target*	AMVO Target	AMVO Phase 3	ANSUR 88
Stature (mm)	1755	1753	1751	1756
Body Mass (kg)	84.2	77.3	76.7	79.2
Erect Sitting Height (mm)	918	--	911	914

* ANSUR II Pilot Study (Paquette et al. 2009).

Data Source

The data for this analysis were drawn from the Seated Soldier Study (Reed and Ebert 2013), the first large-scale study of soldier posture and body shape in vehicle seating environments. A seated posture analysis was conducted with body landmark location data from a single squad seating condition. The body shape analysis was based on laser-scan data obtained with minimally clad subjects in a range of symmetrical unsupported and supported seated postures.

Objective 1: Posture Analysis for the WIAMan Anthropometry Target

Data Set

Data from 100 men were used for the posture analysis. This is a subset of the data from the Seated Soldier Study, because not all data were available at the time of this

analysis. Stature ranged from 1602 to 1965 mm (mean 1759 mm) and body mass index from 18.2 to 38.3 kg/m^2 (mean 26.7 kg/m^2).

Body Landmark Data in Vehicle Seat Conditions

Soldiers were instructed to sit comfortably in the seat. Lower and upper extremity postures were required to be approximately symmetrical. A FARO Arm coordinate digitizer was used to record body landmark locations defining the seated posture. The posture data for the current analysis were extracted from Condition C01, in which the padded seat back was nominally vertical, the padded seat cushion was nominally horizontal, and the seat height above the floor (measured from SAE J826 H-point) was 450 mm (for more details, see Reed and Ebert 2013). The current analysis was conducted using data from conditions in which soldiers wore their Advanced Combat Uniform (ACU), including boots. No other protective equipment or gear was worn. The soldier donned a five-point harness in each condition after selecting a comfortable posture. Figure 1 shows a soldier in condition C01 with the ACU garb level.

Figure 1. Soldier in Condition C01 and the ACU garb level.

Hardseat Data and Analysis

Additional data obtained in a laboratory hardseat, shown in Figure 2, were used to augment the data from the padded test seat. The hardseat provided access to posterior landmarks, enabling a more accurate characterization of each soldier's pelvis and spine geometry. These data were used to estimate pelvis and spine joint center locations relative to surface landmarks. The relationships between the anterior landmarks accessible in the squad seat and the joints were used to estimate joint center locations in the squad seating conditions. For more details on these calculation procedures, see Reed and Ebert (2013).

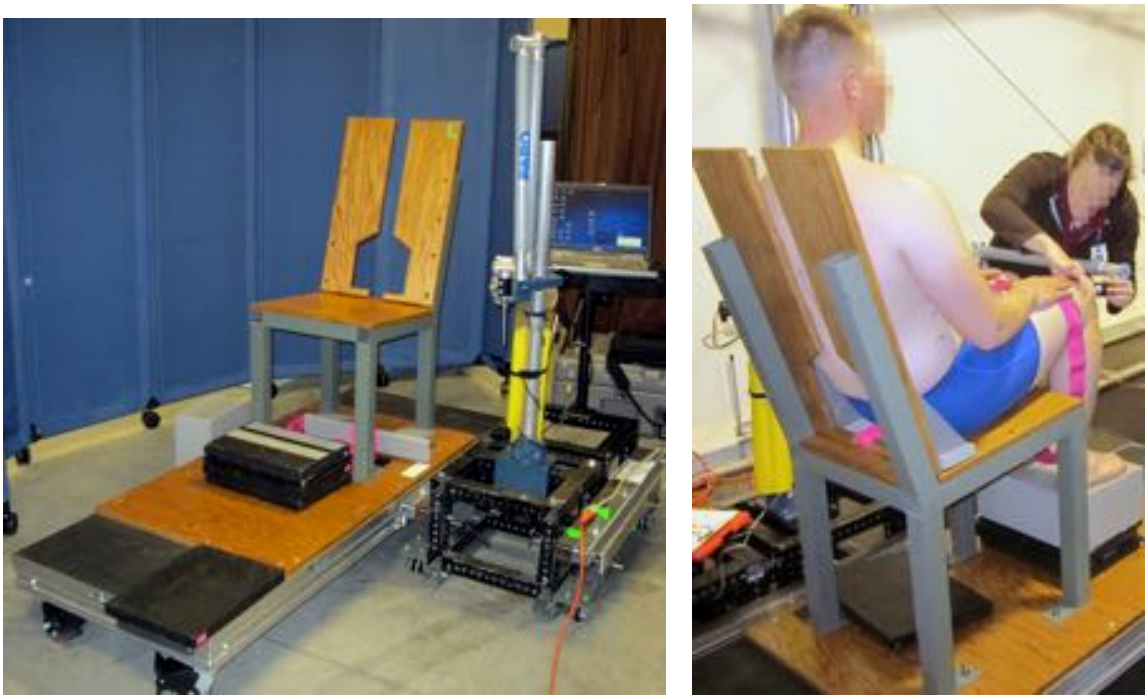

Figure 2. Laboratory hardseat used to obtain additional skeletal geometry information. Note the blue dots on the skin that mark landmarks to be digitized. A nylon strap was used to control leg splay, maintaining the femurs approximately parallel.

Body Landmark and Joint Analysis Methodology

The goal of the landmark analysis was to obtain a consistent set of landmarks and joint center location estimates for individuals who match the reference body dimensions. In most previous analyses of this type (e.g., AMVO), data from individuals judged to be "close" to the reference size were averaged. The current analysis uses a more rigorous regression procedure that allows data from individuals with a wide range of body size to be used. Each landmark or joint coordinate is regressed on stature, body mass index, and the ratio of sitting height to stature. The reference values described above are then input to the resulting equations. To facilitate the interpretation of the analysis, the regressions were performed on principal components (PCs) of the covariance matrix of the landmark coordinates, but all PCs were retained, so the results are equivalent to regression on the individual coordinates. No tests of statistical significance were performed, because excluding non-significant terms would result in inconsistencies across landmarks in trends with body size. For example, BMI was included as a predictor in the regression models for all PCs, even though it was only statistically significant for a few of the PCs.

A rationalization process was applied to obtain symmetrical landmarks. The Y (lateral) coordinates of landmarks on the midline of the body were assigned a value of zero, eliminating small asymmetries, typically less than a millimeter, that remained after the statistical modeling process. Bilateral pairs of landmarks (for

example, left and right acromion) were assigned X and Z values equal to the means of the respective points, and the Y values were set to ± 50% of the initial Y-axis difference between the points.

The output of this analysis and rationalization process was a list of landmark and joint locations that represent the initial target for the WIAMan ATD. As noted below, some additional posture adjustments were conducted to obtain the desired reference posture.

Objective 2. External Body Shape for WIAMan ATD

Laser Scan Data Processing

Laser scan data obtained from minimally clad soldiers were obtained in the Seated Soldier Study. A total of 338 scans from 126 male soldiers were used, with up to four scan postures per soldier (not all soldiers were scanned in all conditions). Due to the study design and limitations in data availability at the time of analysis, this is a different subset of the participants than was used for the posture analysis. Note that the analysis techniques are robust to differences in the samples. Stature ranged from 1584 to 1965 mm (mean 1754 mm) and body mass index from 18.3 to 38.9 kg/m^2 (mean 26.7 kg/m^2). Figure 3 shows the four postures. Surface body landmark locations were extracted from the scan data, as described in Reed and Ebert (2013).

A uniform template mesh developed for this project from a typical scan was fit to each scan so that each scan was represented by a homologous set of 30,004 vertices. (Reed et al. 2014). Figure 4 shows the template, example data with landmarks, the template initially morphed to match the data at a subset of the landmarks, and the result after final template fitting. A principal component analysis (PCA) was conducted on the vertex coordinates. For the subsequent regression analysis to predict body shape, 60 of 126 PCs representing over 99 percent of the variance in the coordinate data were retained.

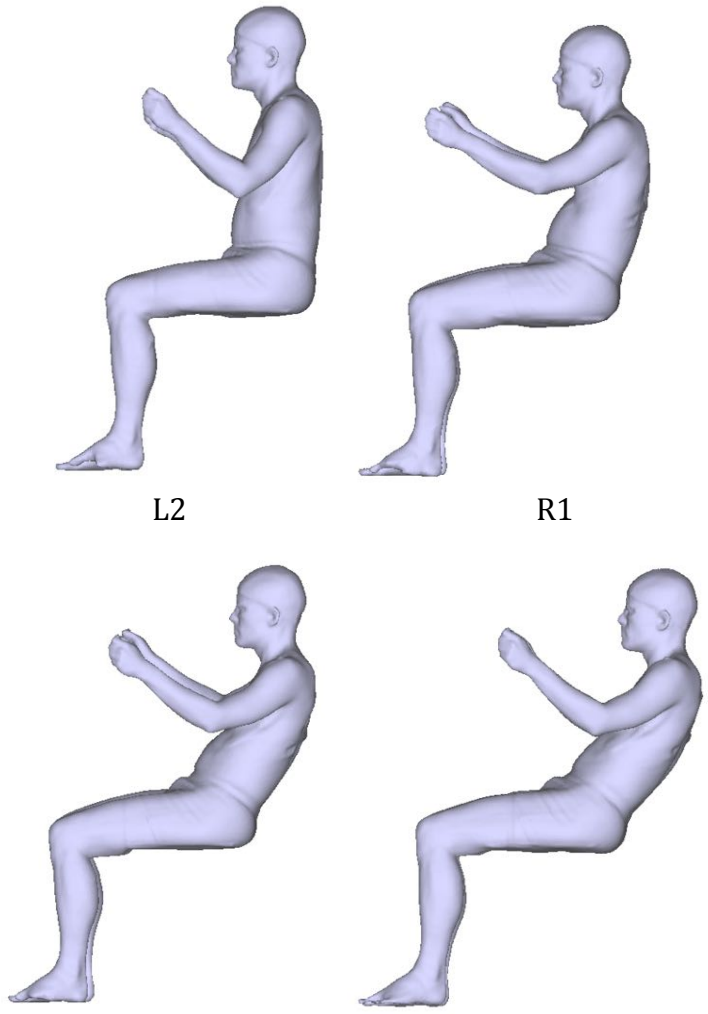

Figure 3. Four subjects in the four scan postures used for the current analysis. Postures R1, R2, and R3 were supported by a small, padded backrest.

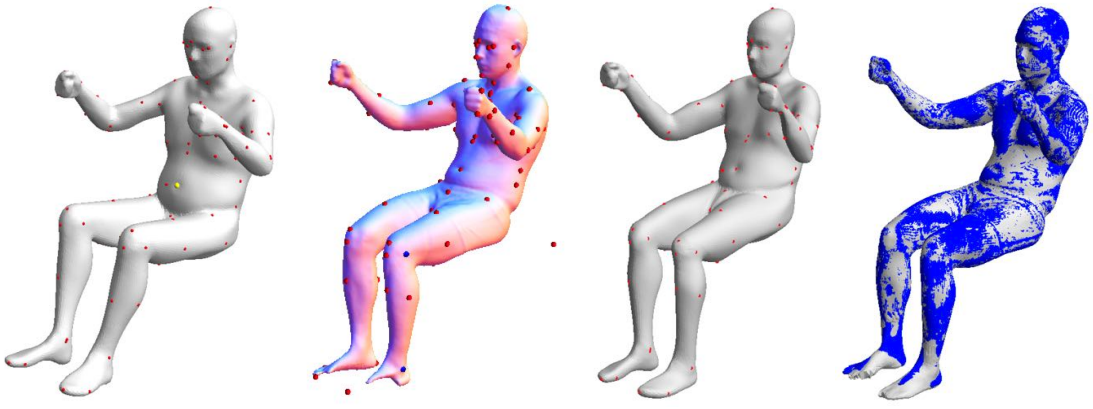

Figure 4. Template with landmarks (A), sample scan with landmarks (B), the template morphed to match the data at individual landmarks (C), and the result of template fitting to the scan (blue, D).

The body shape analysis proceeded somewhat differently from the landmark analysis. One approach would be to conduct a regression analysis to predict PC scores from the reference body dimensions in the same manner as with the landmark data. However, because the scan and landmark data were drawn from different subjects in different conditions, some discrepancies would inevitably emerge. Consequently, a set of landmark joint locations were used along with the body dimensions as input to the body shape predictions. Table 3 lists the landmarks and joints. All landmarks and joints were included in the PCA of the body shape data, enabling verification that the landmark and joint targets were met (all discrepancies < 0.1 mm).

Table 3
Surface Landmarks and Joints Used Along with Stature, BMI, and the Ratio of Sitting Height to Stature To Predict Surface

Glabella_Ct_L	SpineT04_Ct_M
Tragion_Rt_L	SpineT12_Ct_M
Tragion_Lt_L	SpineL03_Ct_M
Suprasternale_Ct_L	L5S1Joint
Substernale_Ct_L	HipJntRt
SpineC07_Ct_M	HipJntLt

Posture Adjustment

The desired design posture for the WIAMan included a horizontal thigh segment and a vertical leg. Because the posture data used to generate the target body shape and landmark locations were obtained with a fixed-height seat somewhat lower than would be required to obtain a horizontal thigh, the initial model was morphed to obtain the desired posture.

Rigid-body rotation matrices were calculated for the foot, leg, and thigh to obtain the desired posture. The deformations at the joints (hip, knee, ankle) were obtained by constructing a global morphing function based on a radial basis function method (Bennink et al. 2007). A cuboid of control points on each segment was rotated to the desired position. The displacements of the control points were used to calculate the morphing function, which was then applied to the vertices of the surface mesh. Landmarks and joints on the upper extremity were also adjusted slightly to match the segment lengths calculated in the squad posture data. Some vertices under the thigh were raised to the buttock plane to create a flat underside to the contour, matching the plane of the flat seat on which the scans were taken.

Spine Joint Interpolation

The surface landmark data were used directly to estimate spine joints at the atlanto-occipital junction, C7/T1, T12/L1, and L5/S1. To provide additional guidance for ATD design, the intervening joint centers, defined as the estimated geometric

centers of the intervertebral disks, were estimated from the surface contour by interpolating between the previously calculated joint centers. The motion segment heights (e.g., L4/L5 to L5/S1) were determined as fractions of the lumbar, thoracic, and cervical chord lengths using data from Black et al. (1991).

Objective 3. Male Pelvis Geometry

The external body landmark measurements obtained in the Seated Soldier study provided good information on the position and orientation of the pelvis, but the data are insufficient to specify the overall size and shape of the pelvis. To provide detailed guidance for ATD design, an analysis of medical imaging data was conducted. The 3D locations of 31 landmarks were extracted from CT studies of 49 men with a wide range of body size. The landmarks from each pelvis were aligned using a Procrustes superimposition and a linear regression was conducted to express the landmark locations as a function of the bispinous breadth (distance between the anterior-superior iliac spine landmarks). Using data from ANSUR 88 (Gordon et al. 1989) the mean expected bispinous breadth for the reference body dimensions is 231 mm (bispinous breadth is not available in ANSUR II). Inputting the target bispinous breadth into the regression model yielded the desired landmark configuration. The landmarks were rationalized by making the left and right sides symmetrical and assigning landmarks on the mid-sagittal plane a lateral coordinate value of zero. The resulting landmark configuration was then translated and rotated to align with joint locations estimated from the surface body landmarks. A generic midsize-male pelvis surface model developed in previous UMTRI research (unpublished) was morphed using radial-basis-function techniques (Bennink et al. 2007) to match the target landmark configuration, providing geometric guidance for the overall bony pelvis and sacrum.

Objective 4. Effects of Gear Ensemble on Torso Posture

The goal of this analysis was to provide guidance on realistic soldier posture for biomechanics testing in support of the WIAMan program. In the previous Seated Soldier Study (Reed and Ebert, 2013), linear regression was conducted to develop statistical models to predict torso posture as a function of seat and soldier variables. The analysis was conducted in two stages using data from the conditions listed in Table 4. First, ACU data from conditions C01, C02, C05, and C07 were analyzed to determine the effects of seat back angle, seat height, and soldier body dimensions on the torso posture. Second, the effects of garb level were quantified in conditions C01 and C05. Garb levels were advanced combat uniform (ACU), personal protective equipment, i.e., body armor vest and helmet (PPE) and "encumbered" with a tactical assault panel with gunner equipment (ENC). The ENC condition includes a hydration pack (see Reed and Ebert, 2013, for more detail.)

Table 4
Crew Trials Used for Regression Analysis of Torso Posture

Condition	Back Angle (deg)	Cushion Angle (deg)	Seat Height (H30)	ACU (N)	PPE (N)	ENC (N)
C01	0	0	450	121	89	87
C02	0	0	350	79	0	0
C05	10	5	450	96	47	47
C07	10	5	350	80	0	0

Objective 5. Relationships Among T12, L5, and S1 Spine Segments and Pelvis

An analysis of medical imaging data was conducted to gain more insight on the relationships among skeletal components than was possible with externally measured data. As part of ongoing UMTRI research, a set of landmarks were extracted from clinical CT scans of 31 men with a wide range of body size. The large range of body dimensions ensures that the regression analysis will produce accurate results for the WIAMan reference body dimensions, which are near the center of the distributions of stature and body weight. Figure 5 illustrates the landmarks, which included points on the inferior and superior margins of the vertebral bodies as well as the anterior-superior iliac spine (ASIS) and pubic symphysis (PS) landmarks on the pelvis. For the current analysis, the orientation of T12 was computed as the normal to the inferior endplate of the vertebral body. The orientation of S1 was calculated normal to the superior endplate. The pelvis orientation was calculated normal to the plane formed by the ASIS and PS landmarks. These orientations, illustrated using 50-mm red lines in Figure 5, were analyzed in conjunction with body segment data measured on soldiers to estimate skeletal component orientations.

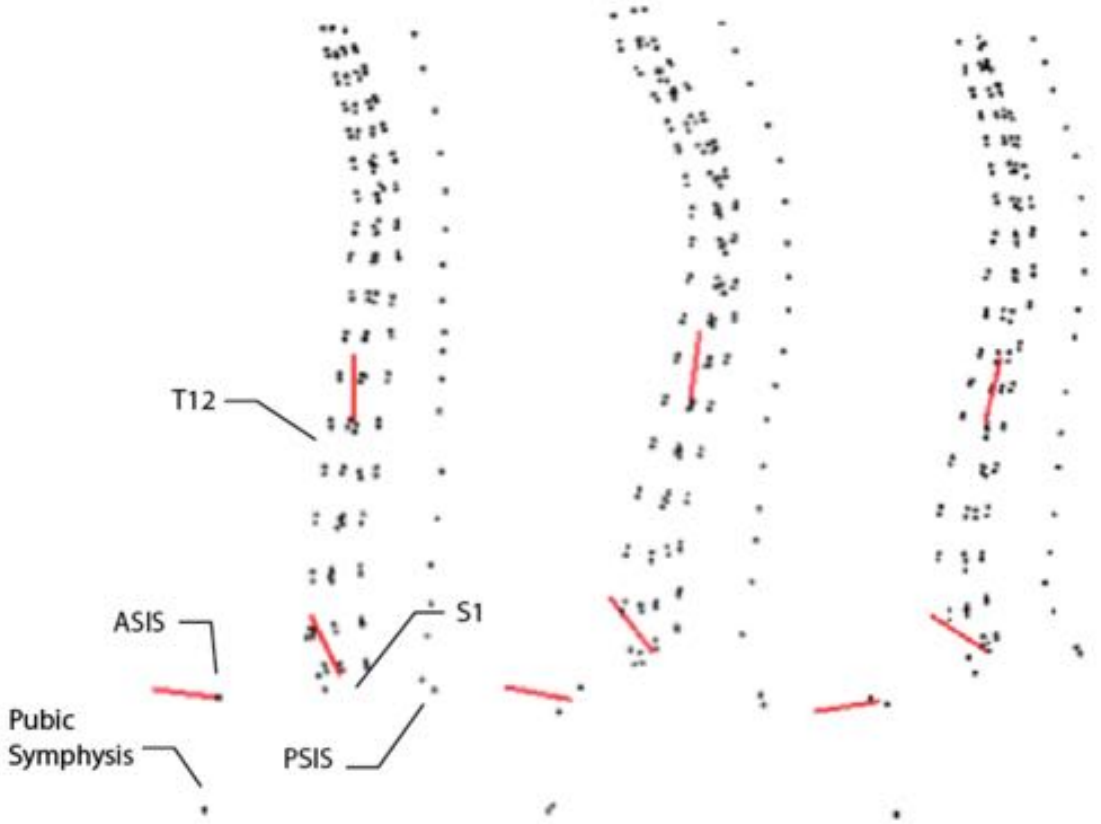

Figure 5. Illustration of landmarks extracted from CT studies. The red lines indicate the orientations of T12, S1, and the pelvis, defined by the normals of the inferior endplate of T12, the superior endplate of S1, and the plane formed by the ASIS and pubic-symphysis landmarks on the pelvis.

Objective 6. Effects of Seat and Soldier Factors on Torso Posture

The posture analysis for Objective 4 was limited to data from a single test condition (squad C01) with the objective of quantifying torso segment orientations across gear ensemble levels in the same test condition used in Objective 1 to define the reference posture for the WIAMan ATD.

Because additional information was needed to support the biomechanics testing being conducted as part of the WIAMan program, posture-prediction models developed during the Seated Soldier Study were extracted from Reed and Ebert (2013) and exercised to develop predictions for specific conditions as a function of seat back angle and ensemble level, using the WIAMan reference body dimensions as input.

RESULTS

Objective 1: Posture Analysis for the WIAMan Anthropometry Target

Landmarks and Joints

Tables 5A-5D list landmark and joint locations calculated using the regression methods described above. The X axis is positive rearward, the Y axis is positive to the right, and the Z axis is positive upward. The origin is an arbitrary point on the midsagittal plane, chosen to allow any landmark to be moved without affecting the others.

Table 5A
Head and Upper Torso Landmarks (mm)

Name	X (fore-aft)	Y (lateral)	Z (vertical
BackOfHead	225.6	0.0	531.2
TopOfHead	127.2	0.0	621.7
Tragion_R	127.2	76.5	489.8
CornerEye_R	53.9	51.7	502.5
Infraorbitale_R	43.0	32.7	490.7
Glabella	24.0	0.0	526.7
Suprasternale	114.7	0.0	292.0
Substernale	83.7	0.0	91.0

Table 5B
Extremity Landmarks and Joints (mm)

Name	X (fore-aft)	Y (lateral)	Z (vertical
AntAcromion_L	135.5	-195.0	320.8
LatHumEpiCond_L	26.6	-352.8	101.1
WristLat_L	-206.6	-392.5	215.0
FemEpiCond_L	-299.6	-149.6	-182.9
Suprapatella_L	-331.7	-110.0	-137.0
Infrapatella_L	-350.0	-103.0	-190.0
LatMall_L	-287.2	-143.6	-595.4
Heel_L	-207.9	-128.5	-686.8
MetaTars5_L	-411.7	-157.7	-681.6
Toe_L	-513.3	-79.6	-681.6
ShoulderJoint_L	164.7	-175.0	278.4
ElbowJoint_L	16.2	-323.8	90.1
WristJoint_L	-201.1	-397.0	244.3
KneeJoint_L	-303.0	-110.1	-177.6
AnkleJoint_L	-303.0	-110.2	-595.5
AntAcromion_R	135.5	195.0	320.8
LatHumEpiCond_R	26.6	352.8	101.1
WristLat_R	-206.6	392.5	215.0
FemEpiCond_R	-299.6	149.6	-182.9
Suprapatella_R	-341.0	110.0	-137.0
Infrapatella_R	-365.0	103.0	-190.0
LatMall_R	-287.2	143.6	-595.4
Heel_R	-207.9	128.5	-686.8
MetaTars5_R	-411.7	157.7	-681.6
Toe_R	-513.3	79.6	-681.6
ShoulderJoint_R	164.7	175.0	278.4
ElbowJoint_R	16.2	323.8	90.1
WristJoint_R	-201.1	397.0	244.3
KneeJoint_R	-303.0	110.1	-177.6
AnkleJoint_R	-303.0	110.2	-595.5

Table 5C
Pelvis Landmarks (mm)

Name	X (fore-aft)	Y (lateral)	Z (vertical
HipJoint_L	120.2	-88.2	-177.6
HipJoint_R	120.2	88.2	-177.6
ASIS_Measured_Surface_R	122.0	113.4	-81.5
ASIS_Measured_Surface_L	122.0	-113.4	-81.5
ASIS_Bone_L	123.8	-115.4	-84.9
ASIS_Bone_R	123.8	115.4	-84.9
PSIS_Bone_L	251.7	-54.8	-160.3
PSIS_Bone_R	251.7	54.8	-160.3

Table 5D
Spine Landmarks and Joints (mm)

Name	X (fore-aft)	Y (lateral)	Z (vertical
C7_Surface	211.7	0.0	382.9
T4_Surface	262.2	0.0	286.2
T8_Surface	296.3	0.0	176.3
T12_Surface	306.1	0.0	59.5
L2_Surface	292.2	0.0	-22.9
L5_Surface	271.4	0.0	-111.2
L5S1Joint	200.0	0.0	-110.8
L4L5Joint	207.1	0.0	-75.4
L3L4Joint	217.1	0.0	-40.8
L2L3Joint	228.3	0.0	-7.3
L1L2Joint	236.0	0.0	26.3
T12L1Joint	240.2	0.0	59.6
T11T12Joint	241.4	0.0	91.4
T10T11Joint	240.1	0.0	121.1
T9T10Joint	236.8	0.0	148.9
T8T9Joint	232.2	0.0	174.8
T7T8Joint	226.3	0.0	199.6
T6T7Joint	219.1	0.0	223.6
T5T6Joint	210.3	0.0	246.5
T4T5Joint	199.8	0.0	267.9
T3T4Joint	187.9	0.0	287.8
T2T3Joint	175.8	0.0	306.7
T1T2Joint	164.3	0.0	324.8
C7T1Joint	153.8	0.0	342.3
HeadNeckJoint*	138.9	0.0	466.4

* Atlanto-occipital joint. See Reed and Ebert (2013) for calculation procedures.

Segment Length Comparison

One consideration in evaluating the current results is a comparison of the segment lengths with other "midsize male" representations. Table 6 lists comparative data from AMVO, the "50th-percentile" Hybrid-III ATD, and SAE J826. Note that the AMVO values differ somewhat from the original publication in Schneider et al. (1983). To provide better comparability with the current work, the joint locations were calculated using the methods in Reed et al. (1999) from the AMVO shell surface landmark locations. Table 6 also includes the segment lengths calculated for the midsize-male WorldSID from the AMVO data (Moss et al. 2000).

The abdomen (lumbar) segment length is shorter than in the WorldSID calculations. At the time the WorldSID calculations were conducted, the external contour of the shell was regarded as being more valid than the pelvis reconstructions from surface landmark measurements. However, the more-rigorous methods for pelvis and lumbar spine reconstruction used in the current study are believed to be more valid than the WorldSID calculations.

The extremity segment lengths in the current work are slightly smaller (about 5%) than the corresponding AMVO dimensions, except that the leg is only 5 mm different from WorldSID. For the lower extremity, additional comparison values from the midsize-male Hybrid-III ATD and the SAE J826 values for midsize-male were tabulated. The current values lie between those two sources.

Table 6
Segment Length Comparison (mm)

Segment	Definition	Current	AMVO†	AMVO/WorldSID	Hybrid-III*	SAE J826
Neck	AO-C7/T1	125	117	119		
Thorax	C7/T1-T12/L1	314	305	304		
Abdomen	T12/L1-L5/S1	156	150	192		
Pelvis	L5/S1-mean hip joint center	104	105	89		
Thigh	Hip-Knee	424	447	433	414	432
Leg	Knee-Ankle	418	438	413	401	418
Arm	Glenohumeral-Elbow	282	294	293		
Forearm	Elbow-Wrist	276	278	272		

* From FMVSS 208.
† Joint locations in AMVO were calculated from the midsize-male shell landmark locations reported in Schneider et al. (1983) using methods from Reed et al. (1999) for improved consistency with the current methods.

Objective 2. External Body Shape for WIAMan ATD

Figure 6 shows examples of the range of body shapes that the statistical model can produce. Stature and body mass index were varied to produce these figures. The figure illustrates that the model is capable of simulating a wide range of body shapes, with the WIAMan target lying close to the center of the underlying data.

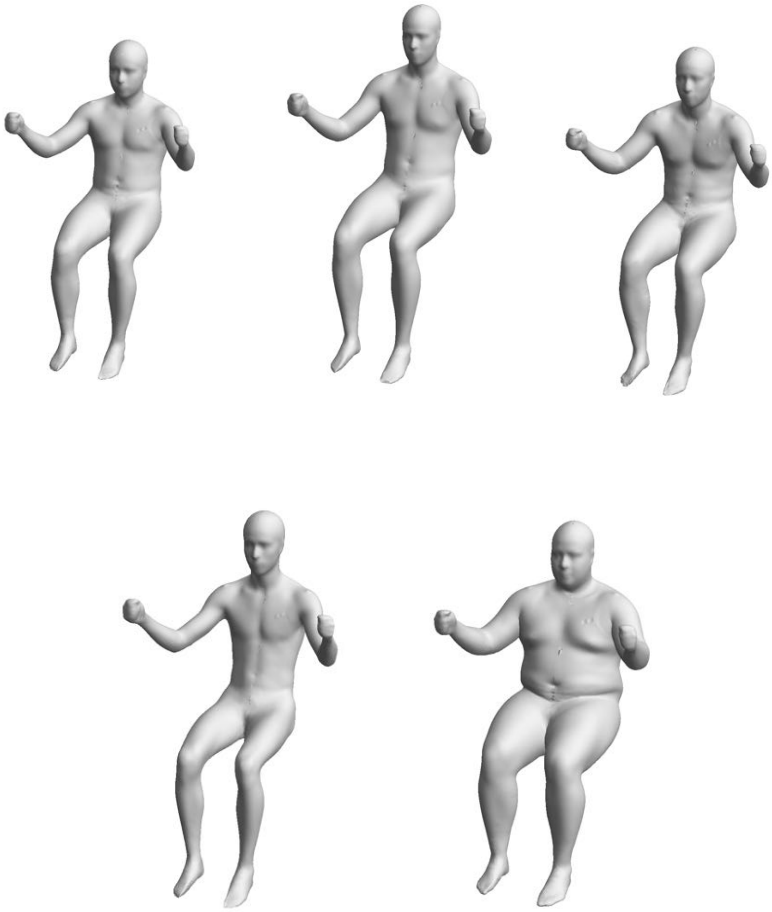

Figure 6. Some of the body shapes that can be produced by the statistical model. The upper right figure is the midsize male body shape obtained using the reference body dimensions (see Figure 7).

Figure 7 shows the body shape and surface landmarks output from the regression model after inputting the WIAMan reference body dimensions, before any adjustments. Figure 8 shows the final body shape, landmarks, and joints following the posture and buttock-shape adjustments. Note that due to limitations of the scanning methodology, the foot geometry is not well represented. The feet depicted in Figure 7 are somewhat smaller than the true foot dimension. Consequently, a

separate study was conducted to develop target foot geometry for WIAMan (Reed et al. 2013).

Figure 7. Body shape output from the regression model prior to posture and shape adjustments.

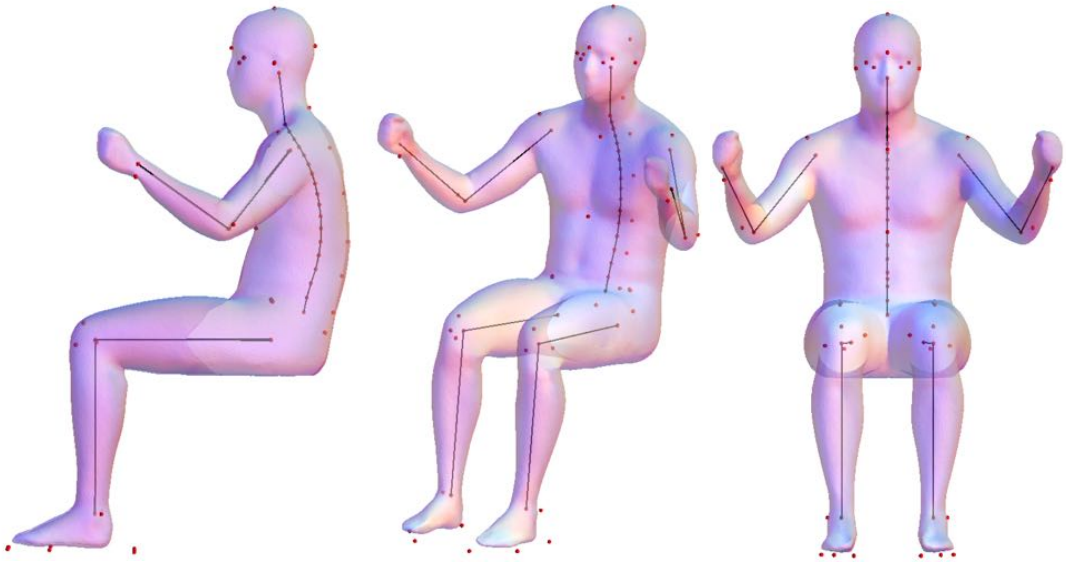

Figure 8. Final body shape with landmarks and joints following posture and contour adjustment. Note that foot landmarks are on perimeter of boot. See Tables 5A-5D for quantitative information on landmark and joint locations.

Figure 9 shows an overlay of the AMVO midsize-male shell with the current body shape. The extremity postures are different but the overall size and shape are similar in both the extremities and torso.

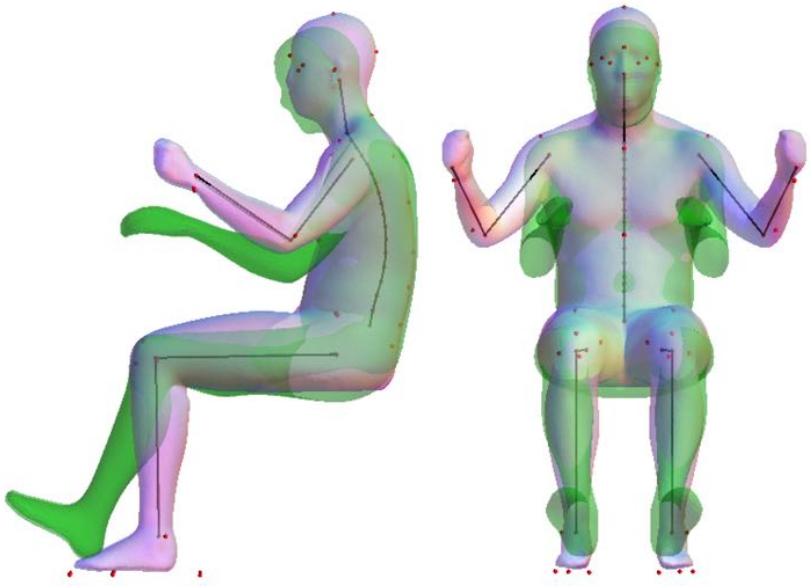

Figure 9. Overlay of current midsize male body shape with AMVO midsize male (green). The AMVO figure is rotated forward 13 degrees from its original position, which represents a typical passenger-car driving posture.

Objective 3. Male Pelvis Geometry

Table 7 lists the pelvis landmark locations in the WIAMan design position. Figure 10 illustrates the pelvis alone and in position inside the shell.

Table 7
Pelvis Landmark Locations (mm)*

X	Y	Z	Name
240.0	-87.0	-83.6	LIliocristaleSum
240.0	87.0	-83.6	RIliocristaleSum
176.8	-140.5	-83.3	LLatIliacWing
176.8	140.5	-83.3	RLatIliacWing
251.3	-43.5	-160.1	LPSIS
251.3	43.5	-160.1	RPSIS
123.8	-115.5	-84.9	RASIS
123.8	115.5	-84.9	LASIS
182.0	0.0	-120.4	AntSupSacrum
216.9	0.0	-114.4	PostSupSacrum
197.5	-22.5	-113.8	LSupSacrum
197.5	20.6	-113.8	RSupSacrum
69.7	-4.1	-161.7	LSupSymphPole
69.7	4.1	-161.7	RSupSymphPole
63.1	-9.0	-157.4	LAntSymphPole
63.1	9.0	-157.4	RAntSymphPole
98.1	-45.1	-240.9	LLatTuberosity
98.1	45.0	-240.9	RLatTuberosity
100.2	-45.2	-247.3	LInfTuberosity
100.2	45.2	-247.3	RInfTuberosity
173.5	0.0	-240.1	AntCaudion

* Origin is an arbitrary location on midsagittal plane. X is fore-aft, Y is lateral, Z is vertical.

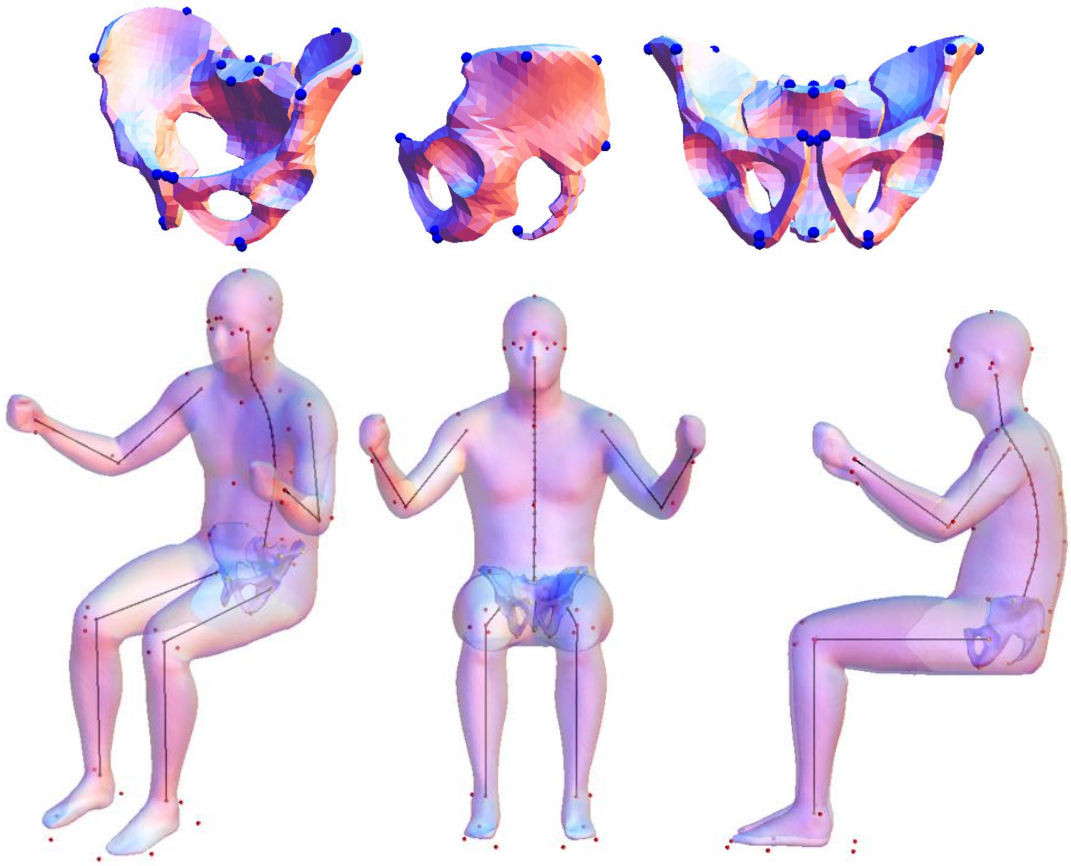

Figure 10. Target pelvis geometry. Note foot landmarks are on boot.

Objective 4. Effects of Gear Ensemble on Torso Posture

Overview

This section provides the results of data analyses that were conducted separately from those that were used to generate the anthropometry target described above. This section uses a larger set of data from C01, including all three gear ensemble levels, and hence the results for the ACU condition differ slightly from those obtained for Objective 1.

Torso Segment Orientations in Posture Data

Figure 11 shows a side-view plot of hip, L5/S1, T12/L1, C7/T1, and head/neck (atlanto-occipital) joint location estimates for men in the ACU garb level in condition C01. The plots show generally similar postures, but a substantial amount of variance in body segment angles and in the overall size of the torso.

Table 8 lists the means and standard deviations of segment angles in condition C01. The variance in cervical and lumbar spine flexion is quantified using the difference in head and thorax angles (cervical) and thorax and pelvis angles (lumbar). Slightly

greater lumbar spine flexion was observed in the ENC condition, but the difference from the ACU condition is less than half of the within-condition standard deviation.

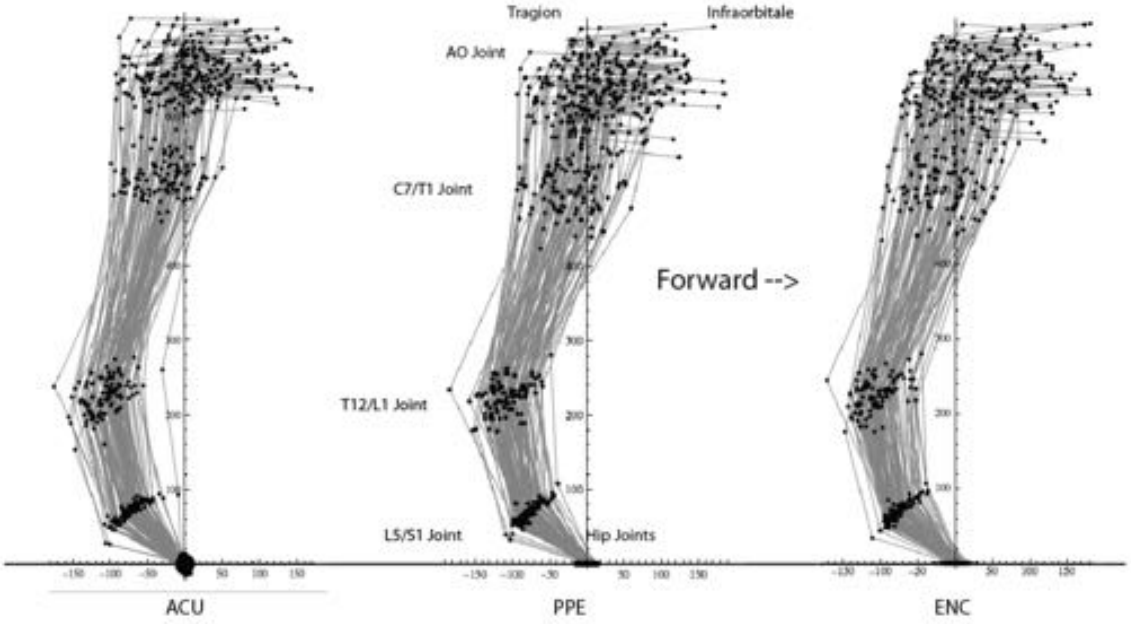

Figure 11. Side-view illustration of torso linkage for men in ACU, PPE, and ENC conditions. Data have been aligned on mean hip joint location.

Table 8
Mean (SD) for Male Torso Segment Angles in Condition C01 (deg)

Segment Angle with respect to Vertical*	ACU (N=100)	PPE (N= 92)	ENC (N=92)
Head (Frankfurt Plane above Horizontal)	1.7 (6.4)	-0.2 (5.8)	0.2 (4.7)
Neck (C7/T1 to AO)	-6.2 (5.1)	-6.8 (5.8)	-7.7 (5.8)
Thorax (T12/L1 to C7/T1)	-14.5 (5.9)	-17.5 (5.9)	-17.9 (6.5)
Abdomen (L5/S1 to T12/L1)	11.6 (5.1)	11.5 (6.1)	10.5 (6.1)
Pelvis (Mean hip to L5/S1)	45.7 (11.7)	49.2 (10.3)	47.5 (11.1)
Cervical Flexion (Head minus Thorax)	16.2 (8.9)	17.7 (8.6)	18.2 (8.0)
Lumbar Flexion (Pelvis minus Thorax)	60.2 (13.7)	66.6 (10.9)	65.4 (12.4)

* Angles are positive reward of vertical

Spine Segment Orientations

The orientations of individual spine segments can be estimated from these data using constant offsets. On average, the orientation of T1 (defined as vector connecting the geometric centers of the endplates) is 14 degrees *forward* (negative)

from the thorax segment orientation. The orientation of T12 is 19 degrees *rearward* of the thorax segment orientation.

Using the mean values from Table 8 for the ACU condition, the mean orientations of T1 and T12 are -28.5˚ and 4.5˚ (positive is rearward of vertical). For the PPE conditions, the orientations of T1 and T12 are -31.5˚ and 1.5˚.

Pelvis and Sacrum Orientations

Figure 12 shows a schematic illustration of a midsize-male pelvis based on calculations conducted for the WIAMan anthropometry analysis. The pelvis segment orientation (hip to L5/S1) is 50 degrees, equivalent to the PPE condition listed in Table 8. For this pelvis orientation, the orientation of the front plane of the pelvis, defined by the ASIS and pubic symphysis landmarks, is 40 degrees, and the plane defined by the corresponding depressed surface landmarks obtained by firm palpation of the landmark is 46 degrees.

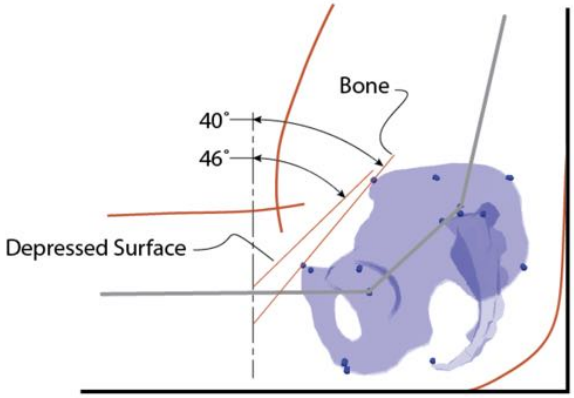

Figure 12. Relative orientation of the pelvis segment (hip to L5/S1), superior sacrum, and front pelvis planes (bone and depressed surface) based on calculations for WIAMan. The segment from hip to L5/S1 is 50 degrees to vertical.

The S1 orientation in Figure 12, which is based on a single pelvis, the normal to the superior surface of the S1 body is oriented approximately 10˚ forward of vertical. Hence, the S1 angle is 50˚ less than the angle of the front plane of the pelvis. However, the CT data analysis provides a broader view of the distribution of S1 orientations.

Objective 5. Relationships Among T12, L5, and S1 Spine Segments and Pelvis

Sacrum Orientations

The CT data (examples shown in Figure 5) were gathered from supine scans. Consequently, the spine segment orientations were adjusted to estimate the spine orientations in the postures represented by the values in Table 8. The analysis considered the orientations of T12, S1, and the pelvis. First, the spine and pelvis

were rotated as a unit to set the orientation of T12 to 4.5˚ or 1.5˚, the mean values for the ACU and PPE conditions (corresponding to thorax segment orientations of -14.5˚ and -17.5˚). Second, the pelvis and sacrum were rotated as a unit to achieve the pelvis segment orientations in Table 8 (45.7˚ and 49.2˚ for ACU and PPE), using the 10˚ offset between the pelvis front plane and the segment. Table 9 shows the results. On average, the sacrum orientation is 49.4˚ greater than the pelvis front plane orientation, giving an estimated mean sacrum orientation of -4.9˚ and -1.4˚ for the ACU and PPE conditions. Relative to the supine condition, the mean T12 and S1 orientations correspond to an average lumbar spine flexion of 38.0˚ and 44.4˚ for the ACU and PPE conditions.

Table 9
Mean (SD) of Male Segment Orientations in Degrees with Respect to Vertical (N=31)

Segment	Supine*	Adjusted to ACU†	Adjusted to PPE†
T12	6.3 (4.8)	4.5 (fixed)	1.5 (fixed)
S1	-41.0 (11.2)	-4.9 (10.6)	-1.4 (10.6)
Pelvis (Hip to L5/S1)	-80.4 (5.5)	45.7 (fixed)	49.2 (fixed)
Pelvis (Front Plane)	-90.4 (5.5)	35.7 (fixed)	39.2 (fixed)
Lumbar Flexion re Supine	--	38.0 (8.9)	44.4 (8.9)

* These angles are expressed with respect to the longitudinal scan axis, equivalent to vertical in the soldier posture data.
† These angles are adjusted by setting the T12 and pelvis frontal plane orientations to the values from Table 8. See text for methodology.

Pelvis and Femur Orientations

Femur angle might be expected to affect pelvis angle through the action of muscles that cross the hip joint. Figure 13 shows the right femur angle with respect to horizontal for 100 men in the ACU condition along with the corresponding pelvis angles. The figure demonstrates that there is no meaningful relationship between these variables. In this test condition, the seat height was fixed and the leg segments were approximately horizontal, so thigh angle is determined primarily by lower extremity dimensions. Hence, this analysis does not assess whether changing thigh angle effects pelvis angle for any individual.

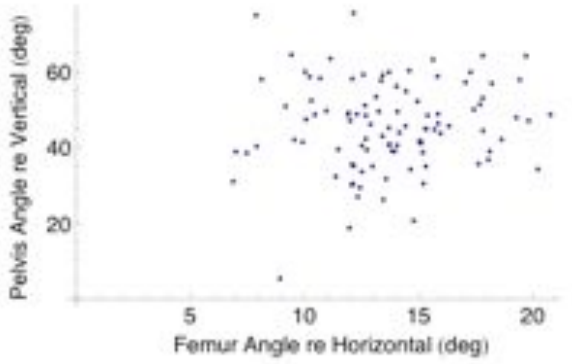

Figure 13. Right femur angle with respect to horizontal versus pelvis angle for 100 men in a single test condition with a 450-mm seat height.

Objective 6. Effects of Seat and Soldier Factors on Torso Posture

The preceding analysis for Objective 3 was conducted using data from a single test condition (squad C01) in the Seated Soldier Study. To provide more information on soldier posture across seating conditions, regression models developed in Reed and Ebert (2013) based on data for the conditions in Table 4 were extracted from the Seated Soldier Study report. Table 11 shows results based on a regression analysis of data from four test conditions at both the ACU and PPE garb levels. The torso segment angles are defined as in Table 8 and the predictors are defined in Table 11.

Table 10
Regression Models* Predicting Crew Torso Segment Posture in ACU†

Dependent Measure	Constant	HipEye Angle	H30	Stature	ln(BMI)	Sitting Height/ Stature	R^2_{adj}	RMSE
HeadSegmentAngle	-55	0.334	--	0.012	--	70.4	0.07	5.9
NeckSegmentAngle	-2.7	0.637	--	--	--	--	0.24	4.6
ThoraxSegmentAngle	-5.9	1.32	--	--	--	--	0.53	5.0
AbdomenSegmentAngle	74.0	1.03	--	--	-17.3	--	0.15	10.5
PelvisSegmentAngle	9.8	0.791	-0.042	--	19.1	--	0.17	10.7

* Assemble the linear function by multiplying each predictor by the associated slope and adding the constant. For example, neck segment angle = -2.7 + 0.637*HipEyeAngle.
† Dependent measures are defined in Table 6, predictors in Table 9.

Table 11
Regression Predictors

Predictor	Definition
HipEyeAngle	Angle of side-view vector from the mean hip joint center to the mean eye location (deg)
H30	Seat height using SAE J1100 definition; height of SAE J826 H-point (also Seating Reference Point for this fixed seat) above heel rest surface (mm)
A40	Seat back angle using SAE J1100 definition; angle of the torso of the SAE J826 manikin with respect to vertical (deg)
Stature	Erect standing height without shoes (mm)
ln(BMI)*	Natural log of body mass index. BMI is calculated as body mass in kg divided by stature in meters squared. ($\ln(kg/m^2)$)
Sitting Height/Stature (SH/S)	Ratio of erect sitting height to stature (mm/mm)

* The natural log transform is used to obtain a distribution closer to normal.

HipEyeAngle is an overall measure of torso recline that is used as an intermediate variable in these posture prediction models. Table 12 lists regression models for HipEyeAngle and for the fore-aft and vertical mean hip joint center location with respect to seat H-point (HipReHPtX, HipReHPtZ).

Table 12
Regression Models* Predicting Crew Posture and Position Variables in ACU

Dependent Measure	Constant	H30	A40	Stature	ln(BMI)	SH/S	R^2_{adj}	RMSE
HipReHPtX	185	--	1.73	--	-66.1	--	0.27	20.5
HipReHPtZ	-98	--	--	--	26.6	--	0.08	12.4
HipEyeAngle	4.6	--	0.540	-0.0059	--	--	0.45	3.0

* multiply each coefficient in the table by the value of the column variable, sum, and add the constant.

Garb level (ACU, PPE, ENC) significantly affected the fore-aft location of the hip joints relative to the seat and the overall torso recline as measured by HipEyeAngle, but did not significantly affect torso segment angles after accounting for HipEyeAngle. Consequently, the effects of PPE and ENC relative to ACU can be accounted for using the constant offsets (mm and deg) in Table 13. Adding PPE shifts the hips forward on the seat and rotates the torso forward slightly. ENC adds to both of these effects.

Table 13
Garb Effects re ACU (mm)

Dependent Measure (mm and deg)	PPE	ENC
HipReHPtX*	-29	-72
HipReHPtZ	--	--
HipEyeAngle (deg)	-1.9	-3.4

* Negative values indicate that the hips are further forward of seat H-point than in the ACU condition

Using these regression models, Table 14 shows body segment orientation predictions for a range of seat back angles for midsize-male soldiers wearing PPE at a seat height of 450 mm. Note that due to the experiment conditions (see Table 4), seat cushion angle with respect to horizontal is assumed to be one half of the seat back angle with respect to vertical. Midsize-male anthropometry is defined at the medians from the ANSUR II Pilot Study (Paquette et al. 2009): stature = 1755 mm, body mass = 84.2 kg, erect sitting height = 918 mm.

Table 14 and Figure 14 show results from imposing seat back angles from -20 to +30 degrees. Note that the back angles in the test data are 0 and 10 degrees; angles outside that range are extrapolation. Negative seat back angles are theoretical, and not intended to predict posture with forward-leaning seat backs. Rather, these conditions are intended to simulate forward-leaning, more-slumped postures that a soldier could choose in a seat with a vertical or slightly reclined seat back.

Because all of the models are linear, the changes across columns (seat back angles) are constant. For example, an increase in seat back angle of 10 degrees increases HipEyeAngle by 5.4 degrees across the range of back angles. Although the true posture changes are likely to be somewhat nonlinear across large changes in back angle, previous research suggests that these linear approximations are reasonable, particularly in relation to the between-subject variance that is not accounted for by body dimensions (Reed 2011).

Table 14
Predicted Midsize Male Segment Orientations (degrees positive rearward of vertical) with PPE

	Seat Back Angle (SAE A40, deg)					
Posture Measure	*-20° †*	*-10° †*	0° **	10° **	20° †	30° †
HipEyeAngle	-18.5	-13.1	-7.7	-2.3	3.1	8.5
HipReHPtX	-97.3	-80.0	-62.7	-45.4	-28.1	-10.8
HipReHPtZ***	-10.0	-10.0	-10.0	-10.0	-10.0	-10.0
Head Segment Angle (Frankfurt Plane above Horizontal)	-3.3	-1.5	0.3	2.1	3.9	5.7
Angle of Side-View Vector from AO to Tragion	-30.3	-28.5	-26.7	-24.9	-23.1	-21.3
Neck Segment Angle (C7/T1 to AO)	-14.5	-11.0	-7.6	-4.1	-0.7	2.7
Thorax Segment Angle (T12/L1 to C7/T1)	-30.3	-23.1	-16.0	-8.9	-1.7	5.4
Abdomen Segment Angle (L5/S1 to T12/L1)	-2.2	3.3	8.9	14.4	20.0	25.6
Pelvis Segment Angle (Mean hip to L5/S1)	39.5	43.8	48.0	52.3	56.6	60.8

* Angles are positive reward of vertical, except for Head Segment Angle, which is positive above horizontal.
** Test conditions; *** No effect of seat back angle (see Table 12)
† Extrapolation beyond test conditions. See text regarding conditions in *italics*.

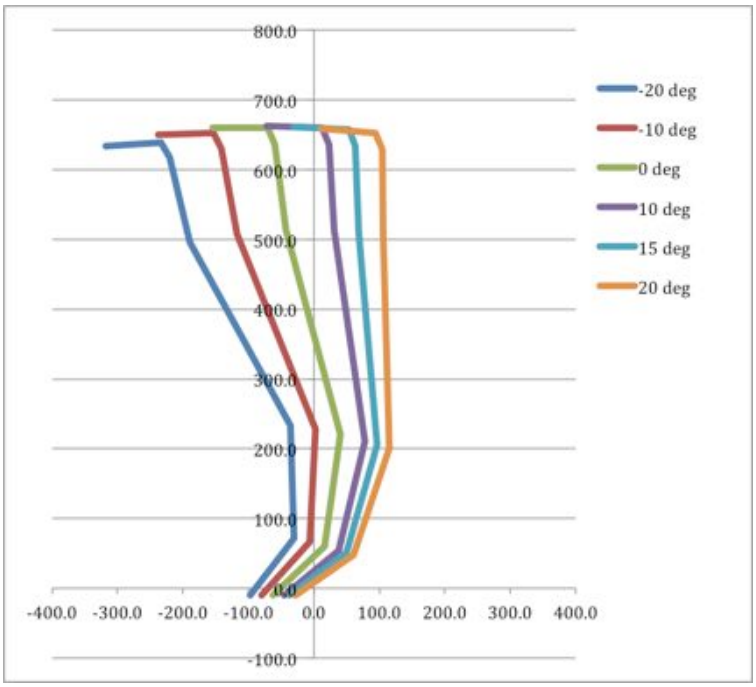

Figure 14. Side-view illustration of predictions from Table 14
(note left-right orientation reversed from Figure 11).

DISCUSSION

This report described the analysis of seated posture and body shape data from soldiers to develop a representative body shape, landmark locations, and joint locations for use in the development of an anthropomorphic test device representing a midsize-male soldier. Note that the ATD may differ from these recommendations due to other design considerations.

Due to limitations in the measurement and analysis methodology, the head, hands, and feet are not representative. In related work, the UMTRI team collaborated with the U.S. Army Natick Soldier Research Development and Engineering Command (NSRDEC) to develop a new head and foot for use in the development of the WIAMan ATD (Reed and Corner 2013, Reed et al. 2013).

The current analysis is the first known application of a three-dimensional regression approach, as opposed to simple averaging, to generate anthropometric specifications for an ATD. The method has strong advantages over simple averaging. For example, it is not necessary that the distribution of anthropometric variables in the study population(s) match the target population. The current analysis used two populations drawn from the Seated Soldier Study for the landmark and body shape analyses that differed somewhat in the means and variances of body dimensions. However, the regression analysis requires only that the underlying data span a reasonable range around the target values, which both data sets do. The models developed for this analysis are most accurate near the center of the distribution (i.e., for the current target values) and would be less accurate for extreme targets (e.g., for creating a "95th-percentile" manikin).

It is also the first known application of a shape model based on whole-body laser-scan data to ATD development. One strong advantage of this approach is that it allows data from subjects with a wide range of body dimensions to be used, simplifying the experimental approach. The method also combined data from landmark measurements on clothed individuals in a realistic seat with whole-body scan data obtained with minimally clad individuals on a test seat. The statistical model linking body shape with landmark locations enabled a realistic body shape to be created for a test condition in which scanning was not feasible.

One important advantage of the current methodology is that the posture and shape models can be exercised to generate accurate predictions for other male body sizes. For example, a "large male" model with 95th-percentile stature and body weight could be readily created. The same methodology could be applied to developing anthropometric specifications for a female manikin, although more data than the 53 women available in the Seated Soldier Study would be needed.

As with all empirical analyses, the current results are limited by the characteristics of the underlying dataset. In particular, the body shape expected for an older, civilian population with the same target body dimensions would be expected to be

somewhat different. However, the substantial similarity between the torso shape of the current model and that of the AMVO midsize-male provides important confirmation that the current results are reasonable and that age-related differences are not likely to be large after accounting for stature and body weight.

The comparison of the body segment lengths with other studies highlighted the lack of definitive guidance on body segment dimensions. After decades of development of human surrogates, the ambiguity persists because of differences in measurement definitions, study populations, and the challenge of estimating joint center locations based on surface landmarks. Nonetheless, the current results are within a few percent of several other widely used representations of midsize men and are undoubtedly sufficiently accurate to represent midsize soldiers for the current application.

REFERENCES

Backaitis, S., and Mertz, H.J., eds. (1994). *Hybrid-III: The First Humanlike Crash Test Dummy*. SAE International, Warrendale, PA.

Bennink, H.E., Korbeeck, J.M., Janssen, B.J., and Romenij, B.M. (2006). Warping a neuro-anatomy atlas on 3D MRI data with radial basis functions. *Proceedings of the 2006 International Conference on Biomedical Engineering*. pp. 214-218.

Black, D.M., Cummings, S.R., Stone, K., Hudes, Palermo, L., and Steiger, P. (1991). A new approach to defining normal vertebral dimensions. Journal of Bone and Mineral Research, 6(8):883-892.

Gordon CC, Churchill T, Clauser CE, Bradtmiller B, McConville JT, Tebbetts I, and Walker RA (1989) *1988 Anthropometric Survey of U.S. Army Personnel: Methods and Summary Statistics*. NATICK/TR-89/044. U.S. Army Natick Soldier Research, Development, and Engineering Center, Natick, MA.

McDonald, J.P., Shams, T., Rangarajan, N., Beach, D., Huang, T-J., Freemire, J., Artis, M., Wang, Y., and Haffner, M. (2003). Design and development of a THOR based small female crash test dummy. *Stapp Car Crash Journal*, 47:551-570.

Mertz, H.J, Jarrett, K., Moss, S., Salloum, M., and Zhao, Y. (2001). The Hybrid III 10-year-old dummy. *Stapp Car Crash Journal,* 45:319-328.

Moss, S. Wang, Z., Salloum, M., Reed, M., van Ratingen, M., Hoofman, M., Cesari, D., Scherer, R., Uchimura, T., and Beusenberg, M. (2000). Anthropometry for WorldSID: A world-harmonized midsize male side impact crash dummy. *SAE Transactions: Journal of Passenger Cars — Mechanical Systems,* 109: 2297-2307.

Paquette SP, Gordon CC, and Bradtmiller B (2009) *ANSUR II Pilot Study: Methods and Summary Statistics*. NATICK/TR-09/014. U.S. Army Natick Soldier Research, Development, and Engineering Center, Natick, MA.

Reed, M.P. (2011). An eyellipse for rear seats with fixed seat back angles. Technical Paper 2011-01-0596. *SAE International Journal of Passenger Cars– Mechanical Systems.* 4(1):586-590.

Reed, M.P. and Corner, B.D. (2013). Generation of a Midsize-Male Headform by Statistical Analysis of Shape Data. Technical Report UMTRI-2013-39. University of Michigan Transportation Research Institute, Ann Arbor, MI.

Reed, M.P., Ebert, S.M, and Corner, B.D. (2013). Statistical Analysis to Develop a Three-Dimensional Surface Model of a Midsize-Male Foot. Technical Report UMTRI-2013-40. University of Michigan Transportation Research Institute, Ann Arbor, MI.

Reed, M.P. and Ebert, S.M. (2013). The Seated Soldier Study: Posture and Body Shape in Vehicle Seats. Technical Report 2013-13. University of Michigan Transportation Research Institute, Ann Arbor, MI.

Reed, M.P., Raschke, U., Tirumali, R., and Parkinson, M.B. (2014). Developing and implementing parametric human body shape models in ergonomics software. *Proc. 3rd International Digital Human Modeling Conference*. Tokyo, Japan.

Reed, M.P., Manary, M.A., and Schneider, L.W. (1999). Methods for measuring and representing automobile occupant posture. Technical Paper 990959. Society of Automotive Engineers, Warrendale, PA.

Schneider, L.W., Robbins, D.H., Pflüg, M.A., and Snyder, R.G. (1983). Anthropometry of Motor Vehicle Occupants: Development of anthropometrically based design specifications for an advanced adult anthropomorphic dummy family, Volume 1. Final report DOT-HS-806-715. U.S. Department of Transportation, National Highway Traffic Safety Administration, Washington, DC.